Ref.TH.2280-CERN

# A SIMPLE MODEL FOR PROTON-ANTIPROTON SCATTERING AT LOW ENERGIES

O.D. Dalkarov *) and F. Myhrer
CERN - Geneva

## A B S T R A C T

The $\bar{p}p$ scattering data at low energies are very well reproduced with the one-boson exchange potential (OBEP) and with the annihilation described by a boundary condition at a certain radius. Our only free parameter is the boundary radius. We show that the elastic $\bar{p}p$ forward peak is not a diffractive peak. Its slope as well as the anti-shrinkage are explained by OBEP alone. We discuss the possibilities of explaining the experimental $\bar{p}p$ resonance within the framework of a potential model.

---

*) On leave from ITEP, Moscow.

Ref.TH.2280-CERN
1 February 1977

## INTRODUCTION

It has been shown that the one-boson exchange potential (OBEP) which fits nucleon-nucleon scattering data, e.g., Ref. 1), predicts many nucleon-antinucleon bound states and resonances [2] (quasinuclear-type states). Experimentally, a bump is found in the $\bar{p}p$ cross-section at 1940 MeV with a width of about 5 MeV [3)-5)]. This bump is a candidate for one of these nucleon-antinucleon resonances. In the dual quark model, one also expects exotic resonances around the $\bar{p}p$ threshold according to the recent arguments presented by Chew [6] and by Veneziano [7].

We will discuss here two questions in the framework of the potential model with $\bar{p}p$ annihilation described by a boundary condition. First we discuss the size of the annihilation region needed to reproduce $\bar{p}p$ scattering data, and second the influence of annihilation on the resonances predicted by OBEP [*]. The last question has been discussed earlier by Myhrer and Gersten [8]. They used the Bryan-Phillips [9] energy-dependent $N\bar{N}$ potential which describes annihilation by an imaginary potential. Myhrer and Gersten showed that when the strength of the imaginary potential was made large enough to fit the observed elastic $\bar{p}p$ cross-section, the $N\bar{N}$ resonances of the real OBEP disappeared. The reason was that the absorptive potential became so strong that it was felt even at large distances (~1 fm). Therefore the absorptive potential strongly modified the scattered wave functions from the pure OBEP result.

Here we will describe the annihilation by a boundary condition so as to avoid the long tail of the absorptive potential of Bryan and Phillips. We will ask the question : which radius $r_c$ of the boundary is necessary to describe the observed elastic and absorptive cross-sections and their energy variation ? Our model is that at the boundary of radius $r_c$ we only have incoming waves, no reflected waves. This model is similar to the one used by Spergel [10]. He assumed only incoming plane waves at the boundary $r_c$ with the effective wave number K at the boundary as an additional parameter. While he needed two parameters to describe annihilation, we will only need one, the boundary radius $r_c$. Further we obtain a simple physical explanation of Spergel's other parameter. Since our NN potential is much better than the one used by Spergel, we get a good description of the experimental $\bar{p}p$ data.

---

*) We will not discuss the $\bar{p}p$ bound states from OBEP in this work.

## THE BOUNDARY MODEL FOR ANNIHILATION

We describe the $N\bar{N}$ scattering by a potential model. The potential is the OBEP taken from Bryan and Scott [1], but with the coupling constants and cut-off parameter as used by Bryan and Phillips [9]. This part of our $N\bar{N}$ model has no free parameters. The parameters in OBEP are all determined from fits to the NN phase shifts.

The $N\bar{N}$ annihilation is described by the boundary condition of Feshbach and Weisskopf [11]. Their idea is simply : at the boundary $r_c$ the scattered wave satisfies a certain condition to be specified. As a consequence it is not possible to obtain any information about the interior ($r < r_c$). The model of Feshbach and Weisskopf assumes only incoming waves at $r = r_c$, i.e., we have no reflections from the boundary.

Using the WKB approximation we can write the wave function at a boundary $r = r_c$ in terms of incoming and outgoing radial waves as

$$u_\ell(r) \sim r\left(h_\ell^{(2)}(Kr) + b\, h_\ell^{(1)}(Kr)\right) \tag{1}$$

where $K$ is the wave number to be defined later. Here $h_\ell^{(1)}(Kr)$ and $h_\ell^{(2)}(Kr)$ are Hankel functions describing outgoing and incoming waves, respectively. Feshbach and Weisskopf say that $b = 0$ in Eq. (1). Further they assume that at the boundary, Eq. (1) with $b = 0$ can be described reasonably well by

$$u_\ell(r) \sim \exp(-iKr) \tag{2}$$

This boundary condition was used by Spergel to describe $N\bar{N}$ annihilation. He used $r_c$ and $K$ as two free parameters to fit data. The effective wave number $K$ was determined such that he had maximum absorption in each partial wave. His condition reads $\partial\sigma_R^\ell/\partial K = 0$ where $\sigma_R^\ell$ is his reaction cross-section for $\bar{p}p$ partial wave number $\ell$.

In our model we use the fact that $K$ is the effective wave number at a distance $r$. We determine $K$ from the value of the OBEP at this point

$$K = \sqrt{M(E - V(r))} \tag{3}$$

where M is the nucleon mass, E is the scattering centre-of-mass energy and V(r) is the one-boson exchange potential at distance r. Since V(r) differs for each partial wave, K will also depend upon the $\bar{p}p$ angular momentum channel [in Eq. (3) we only include the diagonal parts of V(r) for coupled channels]. Generally speaking $V(r) < 0$ for $r_c < 1$ fm. In some angular momentum channels for too small $r_c$, our energy dependent V(r) becomes positive. These small values of $r_c$ will not be needed in our numerical calculations (with our choice of OBEP). However, we will discuss this point in the conclusions.

We have our free parameter in our calculation, $r_c$, which we determine by requiring that our model describes data. We will discuss two boundary conditions : Model I with $u_\ell(r)$ given by Eq. (2) and Model II with $u_\ell(r)$ given by Eq. (1) and $b = 0$. The only relevant input of this wave function is the logarithmic derivative of $u_\ell$ at $r = r_c$. From Eq. (2) we have

$$\left.\frac{u_\ell'(r)}{u_\ell(r)}\right|_{r=r_c} = -iK \tag{4}$$

From Eq. (1) we find Eq. (4) but with a constant depending on $\ell$ multiplying the right-hand side of Eq. (4). Because $Kr_c$ is fairly large (about 2-4), this does not change the right-hand side of Eq. (4) very much for $\ell \leq 3$. Moreover since K does not change very rapidly with $r_c$, i.e., the OBEP does not vary drastically for our values of $r_c$, we can assume that the WKB approximation of $u_\ell$, Eqs. (1) or (2), is good. With the real nucleon-antinucleon OBEP from Refs. 8), 9) and K determined by Eq. (3) we solve the coupled channel Schrödinger equation to obtain the cross-sections.

RESULTS

We will first discuss the results obtained with Model I. We fitted $\sigma_{tot}$, $\sigma_{e\ell}$ and $\sigma_{ex}$ ($ex = \bar{p}p \to \bar{n}n$) vs. energy rather well. The best value of $r_c$ is dependent on the particular $\sigma$ or energy range but it is not a strong function of them. This model did not fit $\sigma$ vs. energy as well as, e.g., the Bryan-Phillips potential model. If we looked at $\bar{p}p$ elastic and charge exchange differential cross-sections, a value of $r_c$ equal to 0.5 fm gave the best results at backward angles. On the other hand, this model did not have a pronounced dip and a second maximum in $d\sigma/d\Omega(\bar{p}p \to \bar{n}n)$ as does Bryan and Phillips' [9].

In Model II we do not find very large differences from Model I. In this case, however, all the cross-sections, vs. energy, are well described by a single boundary radius $r_c = 0.5$ fm (see Figs. 1 and 2) [*]. In addition a more pronounced dip bump develops in $d\sigma/d\Omega$ for $\bar{p}p \to \bar{n}n$ at forward angles. However, we cannot reproduce the data of Bogdanski et al. [12] who find the experimental $d\sigma/d\Omega$ at the dip too high compared to the Bryan-Phillips potential. Since the $\bar{p}p \to \bar{n}n$ cross-section in this experiment is higher than that in other experiments (see Bogdanski et al., Fig. 1), we suspect that a reduction in their value of this cross-section will improve the agreement with theory considerably. Our $d\sigma/d\Omega$ does not differ much from the results of the Bryan-Phillips model as shown in Bogdanski et al. [12] Fig. 2 (see our Fig. 3).

Another interesting fact concerns the forward slope of the $\bar{p}p$ elastic $d\sigma/dt$. At low energies Model II gives $d\sigma/dt$ varying as $\exp(-b|t|)$ for angles up to $60^\circ$ and the value of $b$ can be explained by the OBEP alone. This means the forward peak in $d\sigma/dt$ is <u>not</u> a diffractive peak, but rather the result of a delicate interference between different $\bar{p}p$ partial waves. At these energies the S, P, D and some F waves are the ones that contribute. One does not need higher partial waves to explain the $\exp(-b|t|)$. To be precise we find that for $r_c$ between 0.3 and 0.8 fm the value of $b = 24\ (\mathrm{GeV}/c)^{-2}$, equals the one from OBEP alone, to within 5% at $p_{lab} = 536$ MeV/c. Phillips [13] finds that a pure absorptive potential can describe the forward elastic peak. With our results it is clear that one cannot relate the slope $b$ to the range of the annihilation forces at these energies.

In the Table we show the energy behaviour of $b$ calculated from Model II with $r_c = 0.5$ fm including only points up to $60^\circ$ cm. From these results it is clear that we have an anti-shrinkage of the elastic $\bar{p}p$ forward peak [14]. Figure 4 shows the calculated elastic differential cross-section at two energies from Model II compared with the experimental data from Eisenhandler et al. [15].

---

*) The proton-neutron mass difference is neglected in these calculations.

Finally in Fig. 5 we have plotted the elastic differential cross-section at $180^{\circ}$ as a function of incoming momentum. A clear peak at around $p_{lab} \simeq 0.5$ GeV/c is seen.

## DISCUSSION AND CONCLUSIONS

We have reproduced the $\bar{p}p$ experimental data at low energies with a real one-boson exchange potential plus a boundary (Model II) at $r_c = 0.5$ fm to describe annihilation. The radius $r_c$ is the only free parameter in our calculation.

Our real nucleon-antinucleon OBEP (without annihilation) predicts many $\bar{p}p$ resonances. With an $r_c = 0.1$ fm we still have some OBEP resonances, but they disappear very quickly for increasing $r_c$. With our large value for $r_c$ none survives the annihilation process. The reason is that our boundary condition acts in all partial waves at the same $r_c$. While this assumption has the advantage of simplicity and economy with parameters, it is certainly not a necessary one. In our boundary condition model we can easily see that, e.g., if the OBEP for some angular momenta becomes repulsive for $r \geq r_c$ then the scattered wave might not reach the annihilation boundary and OBEP resonance(s) will remain. For choices of OBEP other than the one we have used this is a real possibility. At this point we should caution that OBEP from nucleon-nucleon scattering is not known at 0.5 fm. More meson exchanges, e.g., $3\pi$ or $4\pi$, must be included in order to extrapolate down to 0.5 fm.

Another possibility to explain the recently confirmed 1940 MeV $\bar{p}p$ resonance [5] is to assume that $r_c$ depends upon the $\bar{p}p$ quantum numbers, i.e., for some values of JLST $r_c$ can be quite small and the arguments about annihilation presented by Shapiro et al [2] will be reasonable (for $r_c \leq 0.1$ fm we do have resonances in this caluclation). We should stress that our $r_c$ is the over-all annihilation radius necessary to fit data which is a rather crude picture of the annihilation. In this work we have made no speculations about a possible $r_c$ channel dependence and a possible fit to the $\bar{p}p$ 1940 MeV resonance.

From our calculations we understand Spergel's boundary condition [10]. His effective momentum can be explained by Eq. (3) and our K is not too different from his parameter. On the other hand, we do not find that K increases with increasing spin J as his parameter does. We ascribe this difference as well as our much better fit to $\bar{p}p$ data to our better NN potential. Spergel's NN potential did not have any explicit $\omega$ exchange which produces a strongly attractive $\bar{p}p$ potential. In fact our fit to the $\bar{p}p$ data is easily comparable in quality to that from the Bryan-Phillips potential [9]. Unlike the Bryan-Phillips optical potential our final numbers only depend weakly on the value of the OBEP cut-off parameter $\Lambda$ [8]. A variation of 10% in this parameter influences our final cross-section very little (see Figs. 1 and 2).

There is, however, one problem that has to be faced in a potential approach to the $\bar{p}p$ scattering. The value of the OBEP for $r \leq 0.8$ fm is typically -1 GeV or deeper. For such a depth relativistic effects must be considered. Further we know from the work of, e.g., Gross [16] that relativistic effects, terms of order $v^2/c^2$, can introduce short-range repulsion in the NN (and therefore also in the $N\bar{N}$ interaction). But to what extent is still an open question [17),18].

We show that the forward $\bar{p}p$ elastic peak is <u>not</u> a diffractive peak and we explain the anti-shrinkage of this peak by means of the OBEP alone. Because several partial waves (S, P, D) contribute to the scattering even at very low energies, one does not expect a $1/v$ behaviour for, e.g., $\sigma_{e\ell}$ and $\sigma_{\text{annihilation}}$.

Further, we show that annihilation occurs at relatively large distances in the $N\bar{N}$ system compared to the Compton wavelength of the nucleon, and generally speaking that it cannot be treated as a perturbation. However, very little is known about the annihilation process itself. Since at least one $N\bar{N}$ resonance has been found, we must understand the annihilation process itself better before speculating how such $N\bar{N}$ resonances succeed in surviving the annihilation. From the quantum numbers of a $N\bar{N}$ resonance (including its mass and width) it is possible to learn more about the short-range behaviour of OBEP. But this requires better knowledge of the coupling of $N\bar{N}$ to meson channels. However, it is surprising that even our crude annihilation model with only one free parameter is able to give a reasonable reproduction of the bulk of the low energy proton-antiproton data.

ACKNOWLEDGEMENTS

We would like to thank Professor T.E.O. Ericson for many stimulating discussions and a critical reading of the manuscript. One of us (O.D.) would like to thank the Theoretical Physics Division for the kind hospitality extended to him.

TABLE

| | | | | |
|---|---|---|---|---|
| $b$ $(\mathrm{GeV}/c)^{-2}$ | 42.7 | 32.6 | 23 | 19 |
| $p_{lab}$ (GeV/c) | 0.218 | 0.310 | 0.536 | 0.73 |

The slope $b$ of the elastic $\bar{p}p$ forward peak $(d\sigma/dt) \propto \exp(-b|t|)$ as a function of lab. momentum is given. The slope $b$ is calculated with our Model II, $r_c = 0.5$ fm and OBEP cut-off $\Lambda = 980$ MeV To find $b$ we only used values of $d\sigma/d\Omega$ between $1.0 \leq \cos\theta^* \leq 0.5$.

REFERENCES


1) R.A. Bryan and B.L. Scott - Phys.Rev. 177, 1435 (1968).

2) I.S. Shapiro - Soviet Phys.Usp. 16, 173 (1973) ;
L.N. Bogdanova, O.D. Dalkarov and I.S. Shapiro - Ann.Phys. 84, 261 (1974) ;
C. Dover - Proceedings of the IV International Symposium on Nucleon-Antinucleon Interactions, Ed. T.E. Kalogeropoulos and K.C. Wali, Vol. 2 (Syracuse, NY, 1975), p. VIII, 37 ;
J.M. Richard, M. Lacombe and R. Vinh Mau - Phys.Letters 64B, 121 (1976).

3) A.S. Carroll, I.H. Chiang, T.F. Kycia, K.K. Li, P.O. Mazur, D.N. Michael, P. Mockett, D.C. Rahm and R. Rubinstein - Phys.Rev.Letters 32, 247 (1974) ;
T.E. Kalogeropoulos and G.S. Tzanakos - Phys.Rev.Letters 34, 1047 (1975).

4) V. Chaloupka, H. Dreverman, F. Marzano, L. Montanet, P. Schmid, J.R. Fry, H. Rohringer, S. Simopoulou, J. Hanton, F. Grard, V.P. Henri, H. Johnstad, J.M. Lesceux, J.S. Skura, A. Bellini, M. Cresti, L. Peruzzo, P. Rossi, R. Bizzari, M. Iori, E. Castelli, C. Omero and P. Poropat - Phys.Letters 61B, 487 (1976).

5) W. Brückner, B. Granz, D. Ingham, K. Kilian, U. Lynen, J. Niewisch, B. Pietrzyk, B. Povh, H.G. Ritter and H. Schröder - CERN Preprint (1976).

6) G.F. Chew - Preprint LBL-5391 (1976) and Talk at the 3rd European Symposium on Nucleon-Antinucleon Interactions, Stockholm (July 1976).

7) G. Rossi and G. Veneziano - Private communications and G. Veneziano Talk at $N\bar{N}$ Workshop, CERN (December 6.8, 1976),

8) F. Myhrer and A. Gersten - Nuovo Cimento, in press.

9) R.A. Bryan and R.J.N. Phillips - Nuclear Phys. B5, 201 (1968).

10) M.S. Spergel - Nuovo Cimento 47A, 538 (1967).

11) H. Feshbach and V.F. Weisskopf - Phys.Rev. 76, 1550 (1949).

12) M. Bogdanski, T. Emura, S.N. Ganguli, A. Gurtu, S. Hamada, R. Hamatsu, E. Jeannet, I. Kita, S. Kitamura, J. Kishino, H. Kohno, M. Komatsu, P.K. Malhotra, S. Matsumoto, U. Mehtani, L. Montanet, R. Raghavan, A. Subramanian, H. Takahashi and T. Yamagata - Phys.Letters 62B, 117 (1976).

13) R.J.N. Phillips - Revs.Modern Phys. 39, 681 (1967).

14) V. Barger and D. Cline - Nuclear Phys. B23, 227 (1970).

15) E. Eisenhandler, W.R. Gibson, C. Hojvat, P.I.P. Kalmus, L.C.Y. Lee, T.W. Pritchard, E.C. Usher, D.T. Williams, H. Harrison, W.H. Range, M.A.R. Kemp, A.D. Rush, J.N. Woulds, G.T.J. Arnison, A. Astbury, D.P. Jones and A.S.L. Parsons - Nuclear Phys. B113, 1 (1976).

16) W. Buck and F. Gross - Phys.Letters 63B, 286 (1974).

17) A. Gersten, R.H. Thompson and A.E.S. Green - Phys.Rev. D3, 2076 (1971).

18) J. Fleischer and J.A. Tjon - Nuclear Phys. B84, 375 (1975).

19) $N\bar{N}$ compilation, Particle Data Group - LBL-58 (May 1972).

20) M. Alston-Garnjost, R. Kenney, D. Pollard, R. Ross, R. Tripp and H. Nicholson - Phys.Rev.Letters 35, 1685 (1975).

FIGURE CAPTIONS

Figure 1 Total and elastic $\bar{p}p$ cross-sections as a function of lab. momentum are plotted. The theoretical curves are all from our Model II, the fully drawn ones calculated with boundary radius $r_c = 0.5$ fm and OBEP cut-off $\Lambda = 980$ MeV ; the dashed curve is for $r_c = 0.5$ fm and $\Lambda = 1100$ MeV and the dashed-dotted one for $r_c = 0.6$ fm and $\Lambda = 980$ MeV. The experimental points are taken from Refs. 3),4). The highest energy points are taken from Ref. 19).

Figure 2 The cross-section for $\bar{p}p \rightarrow \bar{n}n$ as a function of lab. momentum is plotted. See Fig. 1 for details. The experimental points are taken from Ref. 20).

Figure 3 The differential cross-section $d\sigma/d\Omega$ for $\bar{p}p \rightarrow \bar{n}n$ with $\bar{p}$ lab. energy of 250 MeV is plotted. The curve is calculated with Model II and $r_c = 0.5$ fm.

Figure 4 The elastic differential cross-section $d\sigma/d\Omega$ with Model II and $r_c = 0.5$ fm is calculated. The fully drawn line is for $p_{lab} = 0.73$ GeV/c and the dashed line for $p_{lab} = 0.66$ GeV/c. The experimental data points are from Ref. 15) and their $p_{lab} = 0.69$ GeV/c.

Figure 5 The elastic differential cross-section at backward angle, $d\sigma/d\Omega(180^o)$ is plotted as a function of lab. momentum for Model II with $r_c = 0.5$ fm.

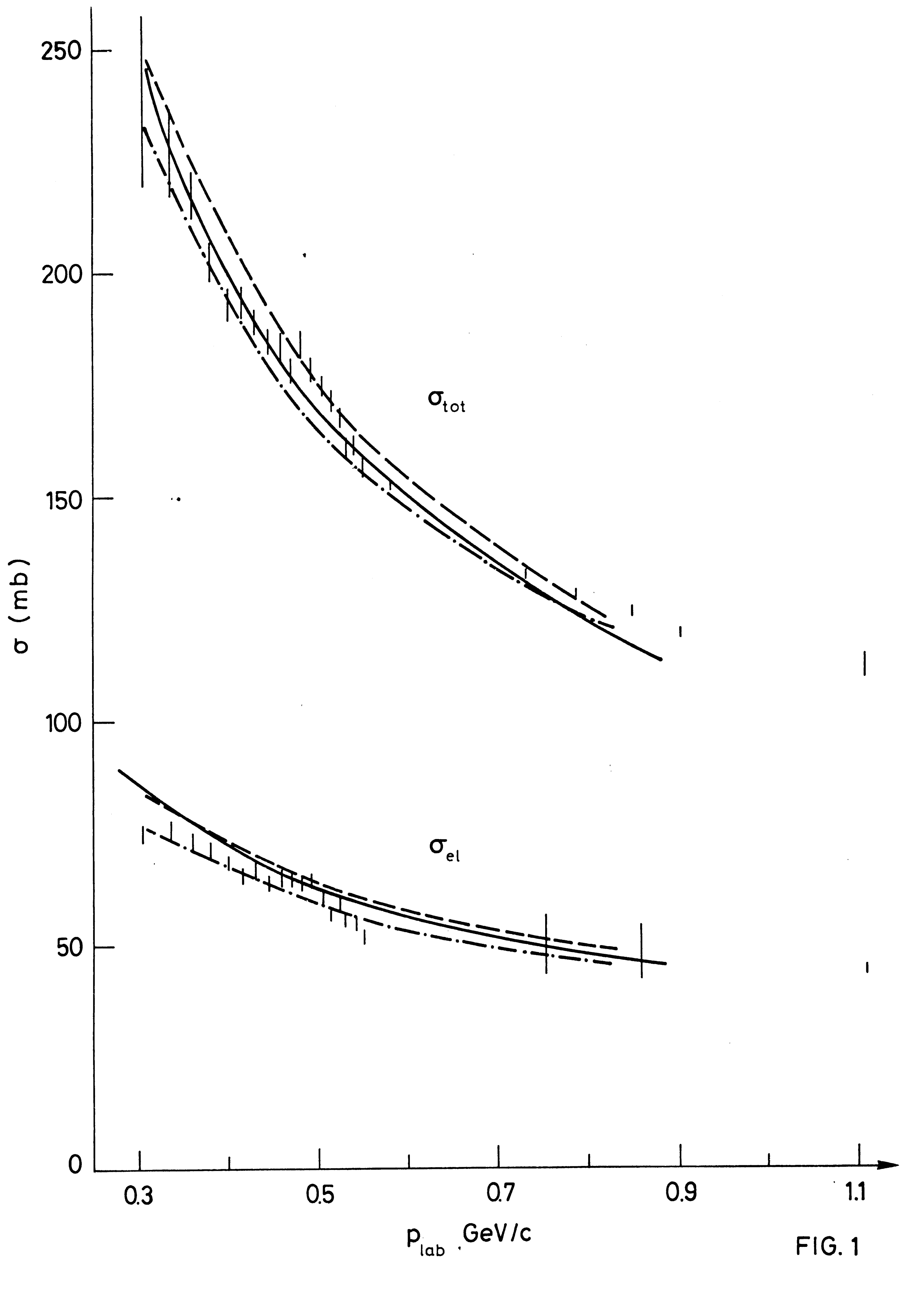


FIG. 1

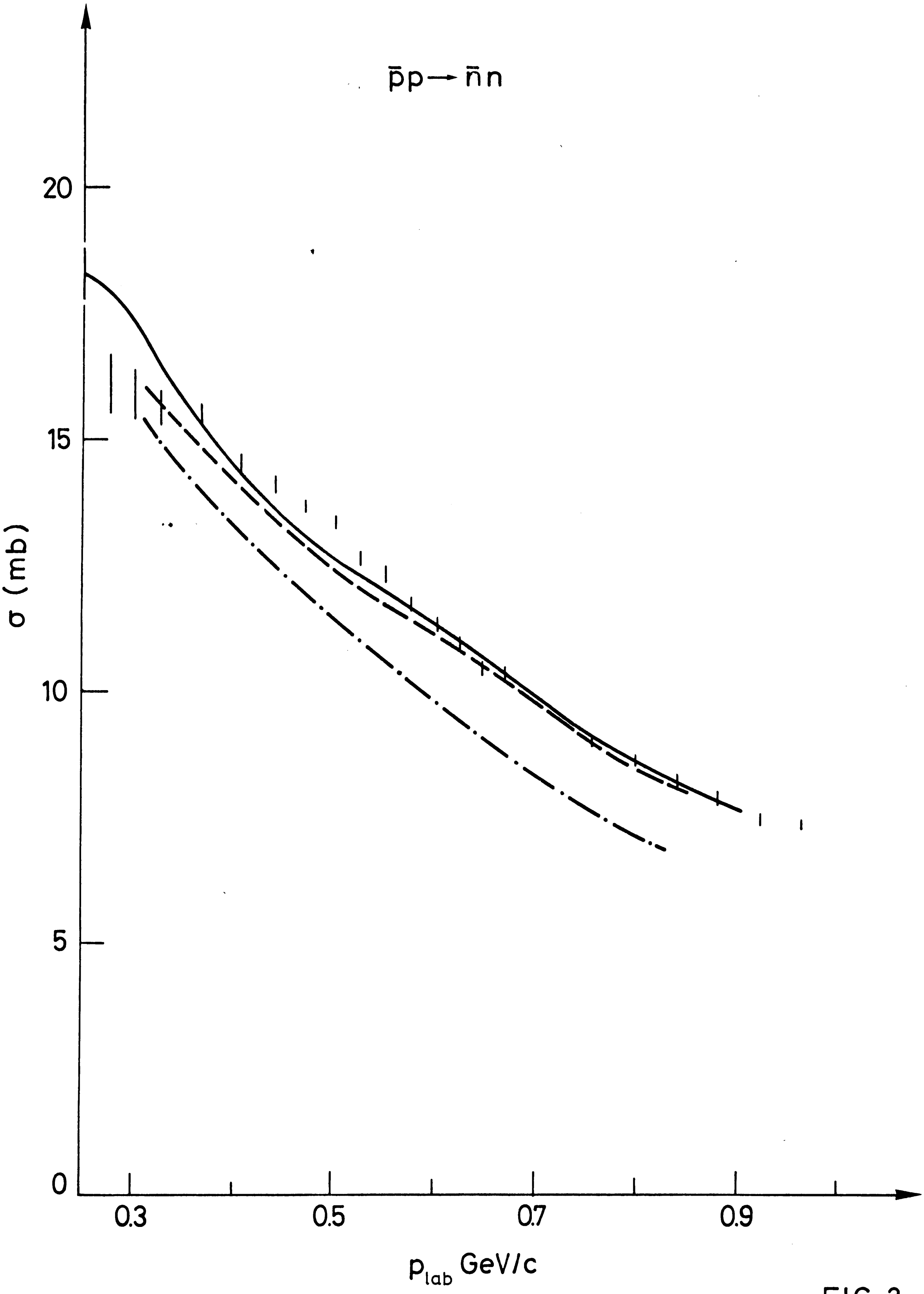


FIG. 2

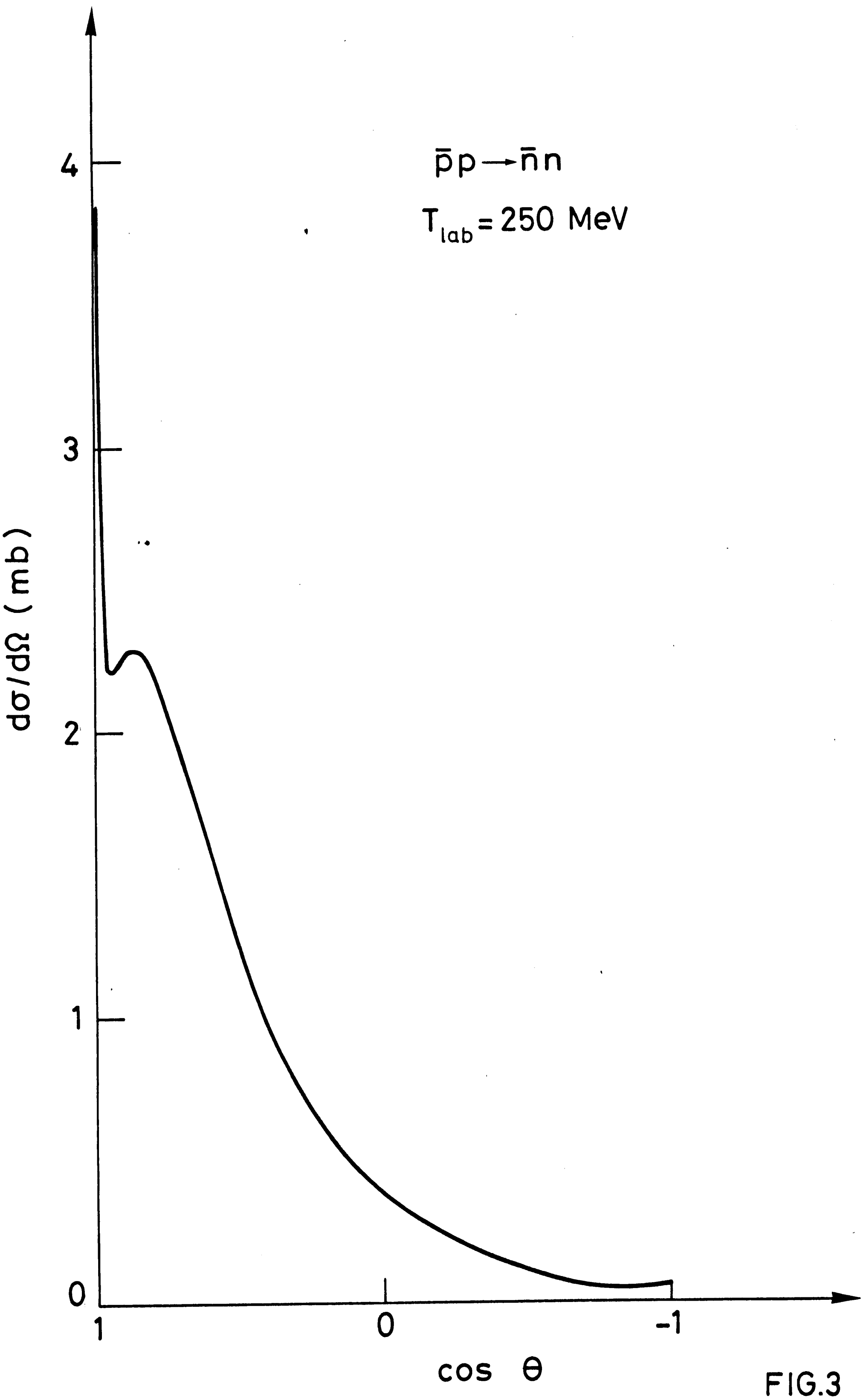


FIG.3

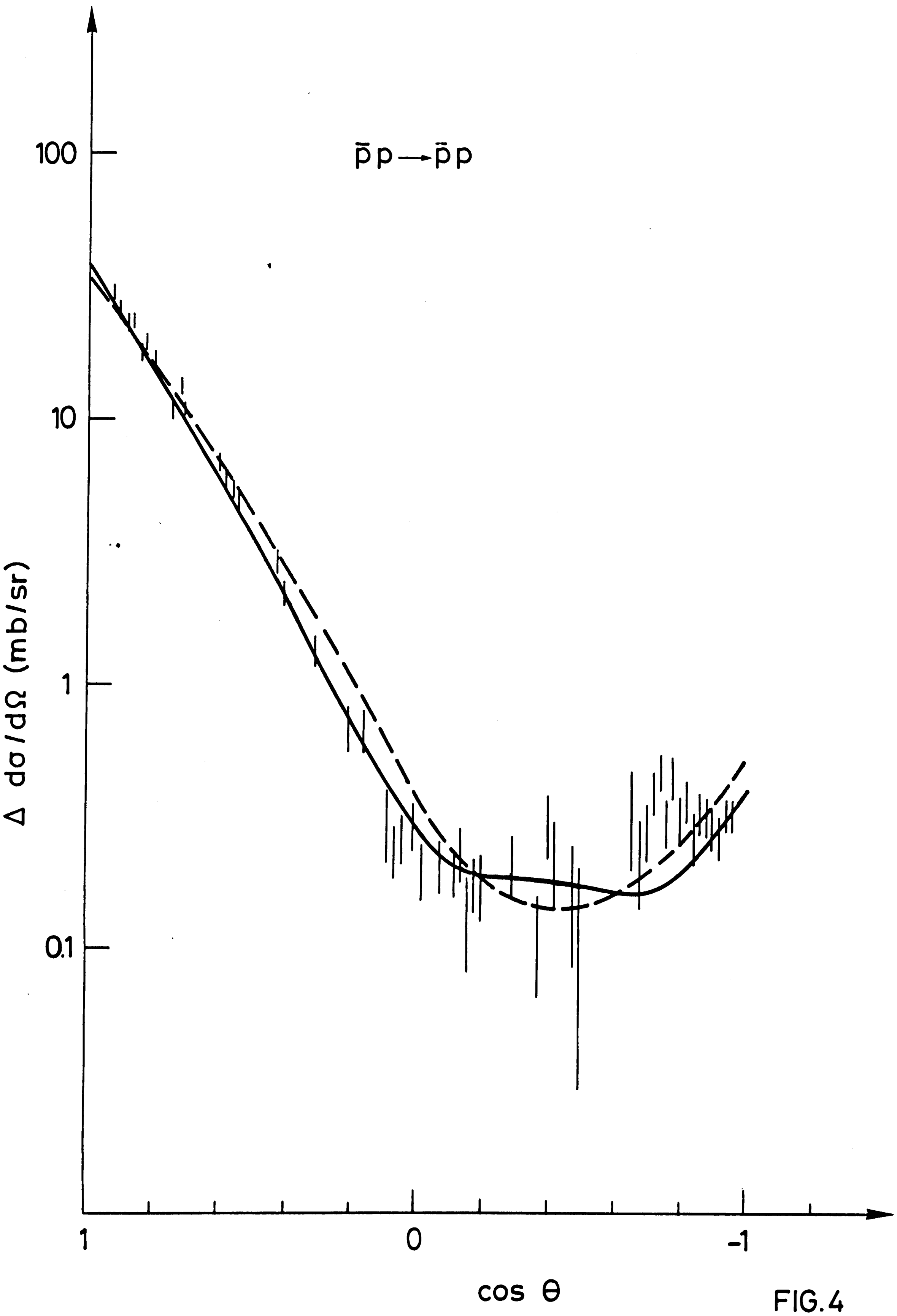


FIG.4

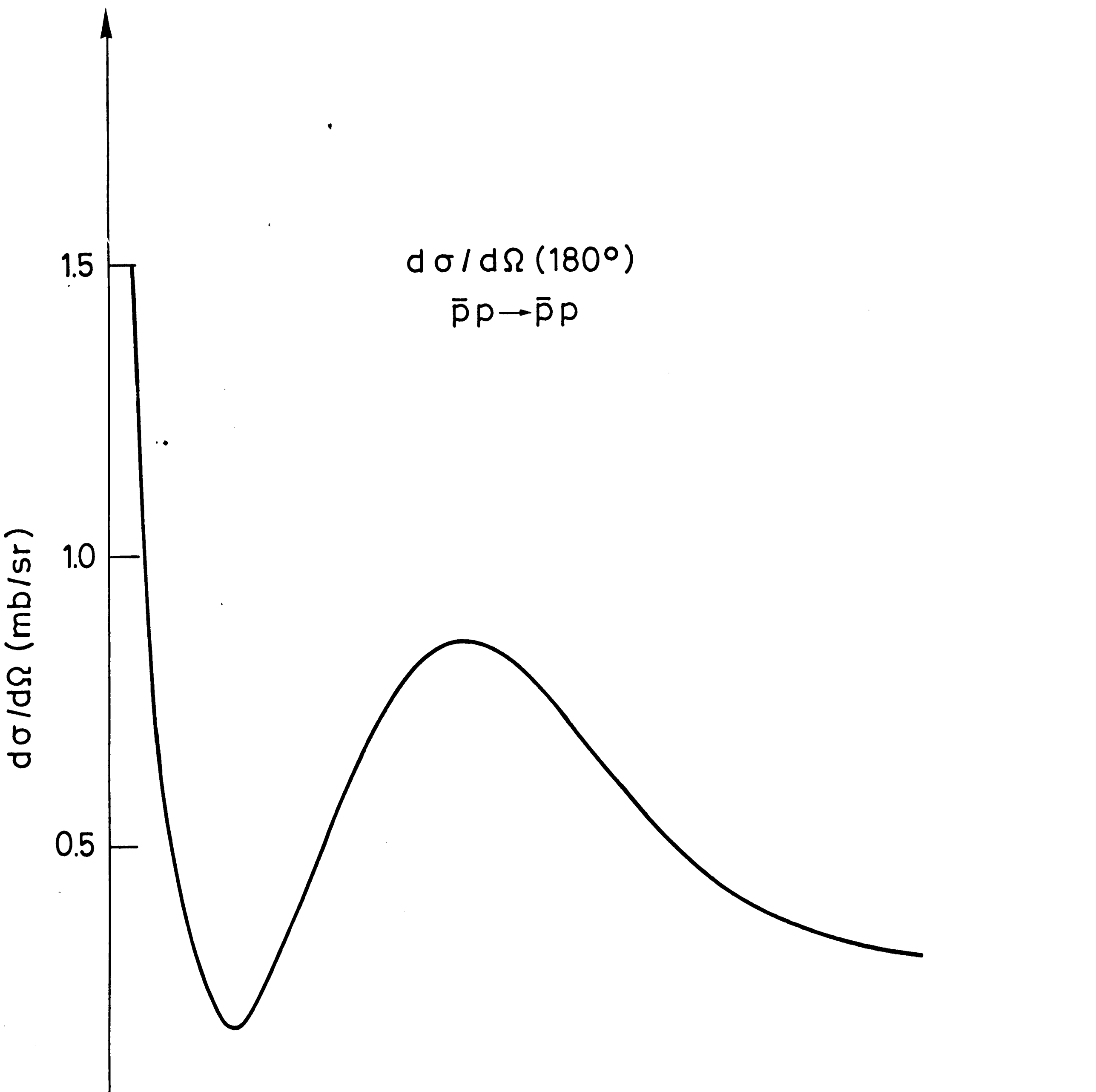


FIG. 5